Model-Based Memory-Efficient Algorithm for Compensation of Toner Overdevelopment in Electrophotographic Printers

Edgar Bernal, Xerox Corporation, Webster, NY; Jan P. Allebach, Purdue University, West Lafayette, IN; Jeff Trask, Hewlett-Packard Company, Boise, ID.

Abstract

Text and line attributes are an integral part of print quality. In this paper, we study artifacts introduced by the electrophotographic process that make text and thin lines with high colorant content appear blurred. We characterize the amount of blurriness of a specific print engine by measuring edge transition widths, and correlate our results with previous psychophysical studies regarding perception of blur to determine the acceptable limits of the printer's performance. We propose a memory efficient algorithm that requires minimal modifications to the printer engine architecture to attain those limits. We demonstrate that the proposed solution outperforms the currently implemented solution in terms of color and texture preservation.

Introduction

Text and line attributes are an integral part of print quality. Multiple efforts have been made to establish the attributes that affect text quality. The ISO/IEC guidelines on hardcopy print quality assessment [1, 2] include print quality metrics for lines and text characters, such as blurriness, contrast, fill, darkness, and raggedness. The INCITS W1.1 ad hoc team [3] defined sub-attributes that compose line quality (line purity, line weight progression, and line color) and text quality (character fidelity, text contrast, and text uniformity). The contribution of these sub-attributes to the perception of overall line quality was also studied [4]. Other efforts have been aimed at designing objective methods for text quality evaluation based on legibility and appearance [5] and on line reproduction quality and modulation transfer function (MTF) [6]. Image quality attributes such as perceived optical density, line width, and tangential edge profile [7], perceived fidelity of line width and edge reproduction [8], and perceived text weight [9] have also been used in establishing the factors that determine text quality. Psychophysical tests were also performed in order to establish detection and discrimination thresholds of blur in edges and lines [10].

The objective of this paper is to study several artifacts introduced in text and lines by the electrophotographic (EP) printing process and to design a memory efficient algorithm that corrects those artifacts. Specifically, we are interested in toner overdevelopment occurring around edges of regions with high colorant concentration. It has been shown that of the six stages of the EP process, the development stage is the one that is mostly responsible for toner overdevelopment [11] which manifests itself in the form of undesired toner particles around edges. The transfer of toner from the developer roller to the photoconductive element exploits Coulomb forces by inducing a charge of the appropriate sign on the toner particles. Consequently, the toner particles will repel themselves in areas where the toner concentration is high, or where there are multiple colorants overprinted on top of each other [11]. There are two different categories regarding the relative positioning of the photoconductive element and the developer roller: In contact printers, as the name indicates, the two components are in contact, whereas in jump-gap printers, there is a small distance between the two. Therefore, in jump-gap printers, the toner particles cover larger distances between the developer roller and the photoconductive element. The toner particles form a chain in the gap region. At the end of the chain, the toner contacts the photoconductor and development occurs. The longer the chain, the more susceptible to particle placement errors the development stage is. This is due to the fact that the influence of the electrostatic, inertial, aerodynamic, and electrodynamic forces increases with the length of the toner chain upon which they act [12, 13]. The placement errors due to toner repulsion or due to the toner chain formation manifest themselves in the form of toner overdevelopment around edges. This appears to the viewer as blurred text and thin-line regions.

The structure of this paper is as follows: we first describe the operation of the image capture devices used to characterize overdevelopment and discuss the image processing techniques used to measure toner scatter. We then describe the memory-efficient algorithm designed to correct overdevelopment around thin edges and text. Lastly, we present some experimental results and give a discussion and the conclusions.

Preprocessing

The procedure for measuring toner scatter consists of printing, scanning, and processing a group of test pages in order to get a metric that quantifies the edge "fuzziness" caused by overdevelopment. Overdevelopment manifests itself in the form of undesired toner particles surrounding thin edges with high concentration of over-printed colorants. Consequently, measurement of the effects of overdevelopment requires not only a high resolution capture device, but also one with good dynamic range. We used the QEA IAS-1000 Automated Image Analysis System[1] whose capture resolution may be set at up to 10,000 dpi (2.54 microns/pixel). It consists of a CCD camera coupled to high resolution optics inside a cabinet with light sources and a positioning stage driven by stepper motors.

Psychophysical Background

The appearance of blurriness correlates to the sharpness of the transition across the line edge from the region where no colorant is present to the interior of the region where colorant is

[1] Quality Engineering Associates Inc, 25 Adams Street, Burlington, MA 01803.

present [14]. The shape of the luminance profile in a direction normal to the line is called the Normal Edge Profile (NEP) [4] and the mean spatial distance over which the NEP goes from 10% to 90% of its luminance range is the Edge Transition Width (ETW) [10]. For the ideal sharp edge, the NEP is a step function; departures from the ideal case may appear to the viewer as blurred edges [4].

Hamerly and Dvorak [10] measured the human visual system's sensitivity to blur in edges and lines under different conditions. They found detection and discrimination thresholds for edges with Gaussian, exponential, and linear normal edge profiles and measured perceived blur in terms of the visual angle subtended by the ETW. They varied the width and contrast ratios of the edges (the ratio between the highest and the lowest luminance values in the stimuli) from 100 to 1.1 and found that sensitivity decreases as luminance ratios increase. (In our case, however, we are only interested in dark edges or, under this definition, edges with high contrast ratios, since toner scatter occurs mainly near regions with high colorant concentration.) They also found that sensitivity is independent of both the shape of the NEP and the line-width. They found detection thresholds (the smallest amount of edge blur that can be reliably detected) to be in the range of 25 to 40 seconds of arc (2.5×10^{-3} in to 4×10^{-3} in at a viewing distance of 20 in), and discrimination thresholds (the smallest difference between the blur of two edges that can be reliably detected) to be on the order of 10 seconds of arc (1×10^{-3} in at a viewing distance of 20 in).

Measuring ETW

A typical test image consists of an approximately vertical line or edge that spans the complete height of the QEA's field of vision, which is equal to 1/10 in at a scanning resolution of 5000 dpi. The procedure for measuring the ETW consists of finding the vertically projected absorptance profile of the captured image and calculating the ETW of that profile.

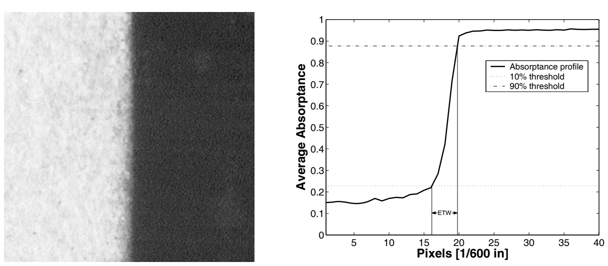

(a) (b)

Figure 1. *Measuring ETW: (a) image of edge (5000 dpi) and (b) projected absorptance profile.*

Figure 1 shows a sample edge scanned at 5000 dpi, its absorptance profile, and the 10% and 90% thresholds used in calculating the ETW. Let P_{min} and P_{max} be the minimum and maximum values of the absorptance profile. The 10% threshold is defined as

$$T_{10} = P_{min} + 0.1(P_{max} - P_{min}), \tag{1}$$

and the 90% threshold is defined as

$$T_{90} = P_{min} + 0.9(P_{max} - P_{min}). \tag{2}$$

As suggested earlier, it has been observed that toner scatter depends on several variables. The scatter measurement tool was used to establish how the value of ETW changes as some of these variables change. For this purpose, we printed several test pages consisting of vertical lines of different widths Ω and different toner concentrations. The length of each line segment was 1/10 in. In this paper, we focus on colorant combinations containing high concentrations of C and M. Figure 2(a) shows how the ETW changes as the width of the line Ω changes while keeping toner concentration constant. In this particular case, the lines had the following combination of colorants: C = M = 100%, and Y = K = 0%. For very thin lines, overdevelopment is not an issue since the amount of toner is too small to cause scatter. The largest amount of scatter occurs at a line width Ω of around 15 pixels. From that point on, as expected, the effect of toner scatter decreases. Figure 2(b) shows the effect of changing the concentration of the C and M colorants while maintaining the line width Ω fixed to 10/600 in. As expected, the effect of toner scatter increases as toner concentration increases.

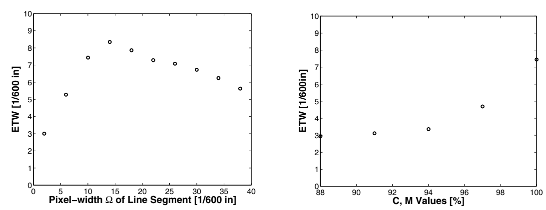

(a) (b)

Figure 2. *(a) Measured ETW as a function of line width Ω: as Ω increases above 15 pixels, ETW decreases. (b) Measured ETW as a function of concentration of C and M colorants: as colorant concentration increases, ETW increases.*

Algorithm for Compensation of Toner Overdevelopment

The objective of the image processing algorithm herein proposed is to reduce toner scatter below the human visual system's detection threshold for edge blur. In current printing products, toner scatter is reduced by limiting the output color gamut of the printer. This is usually done by clipping colorant combinations that are known to cause toner scatter to more conservative mixtures that look as similar as possible to the original combination. This reduction is applied uniformly throughout the image wherever the excessive colorant combinations occur. The result is an overall lightening of these areas of the image. The effect is especially noticeable in large solid areas, where toner scatter is not a problem, and thus clipping is not necessary. In this paper, we propose a spatially varying approach that reduces colorant only where necessary to prevent visible scattering. Elsewhere, the colorant combinations are unchanged. The result is a printed page with color appearance that much more faithfully matches the original print without any colorant reduction. In this sense, the work herein presented is similar to previous efforts oriented towards developing color processing techniques that are dependent on the spatial characteristics of the image [15, 16]. This paper focuses on the HP LaserJet 2605[2] color printer with HP Color Laser Photo & Imaging Glossy Paper. All the data presented in this paper was obtained with this printer and media combination. In addition, the discussion of available hardware resources is also based on the HP LaserJet 2605. However, the methodology reported here is generally applicable to other laser EP printers and paper types as well.

Coring

As seen in the previous section, ETW and consequently perceived edge blur varies as a function of colorant amount and line width Ω. Specifically, edge blur peaks at a specific value of Ω (15/600 in in the case depicted in Fig. 2(a)) and decreases as we move away from that value for a fixed combination of colorants; and it decreases as colorant concentration decreases for a fixed value of Ω (see Fig. 2(b)). Consequently, unless we want to change the spatial characteristics of the image, the only option to decrease the effect of toner scatter is to change the colorant concentration in the regions affected by the unwanted artifact. We chose to implement such a strategy by decreasing the colorant content of the interior portion of lines by a percentage Δ while leaving a 2-pixel edge unmodified, as shown in Fig. 3 for a line with $\Omega = 9$ pixels. Since the shape of the profile results in a decrease of the amount of toner concentration in the central part of the pulse, we will henceforth denote this technique as *coring*.

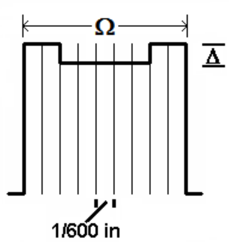

Figure 3. *Shape of proposed line profile.*

In order to verify the performance of the selected line profile, a test page consisting of vertical lines with width $\Omega = 10/600$ in and colorant content C = M = 100%, Y = K = 0% was printed. An edge with width 2/600 in was left unchanged on both sides of the line, and the colorant content in the interior of the line was decreased by different amounts, ranging from 0% to 30% in steps of 2%. The ETW was measured for each of the pulses. Figure 4 shows the results. As expected, ETW decreases as the coring percentage increases.

Optimal Coring

The optimal coring percentage might be defined as the smallest amount of coring that reduces toner scatter below the threshold perceivable by the viewer. Consequently, in order to determine the optimal coring amounts, it is necessary to characterize the behavior of toner scatter with respect to line width Ω, colorant content, and coring percentage Δ for each of the colorant combinations that have been found to produce overdevelopment.

Figure 5(a) shows the measured ETW as a function of coring percentage Δ and line width Ω for the C = M = 100%, Y = K = 0% colorant combination. It can be seen that for very thin lines, toner scatter is not very critical since the amount of toner is not large enough to produce significant scatter. For fixed coring percentage Δ, as line width Ω increases, toner scatter increases to reach its peak at around 15/600 in line width. From this point on, as line width Ω increases, toner scatter decreases steadily. It can also be seen that for a fixed line width Ω, as coring percentage Δ increases, the effect of toner scatter decreases. (For lines whose width is smaller than 5/600 in, it is not possible to leave a 2-pixel wide edge unmodified in the coring process. In these cases, the coring process decreases the colorant content along one of the columns of the line, leaving the rest unchanged.) Due to the limited field of view of the image capture device, line widths beyond 60/600 in were not tested. Figure 5(b) shows, superimposed on top of the data in Fig. 5(a), a flat surface with height equal to the value of the absolute blur detection threshold estimated by Hamerly and Dvorak [10] (40 arcseconds correspond roughly to 4×10^{-3} in or $2.4/600$ in at a viewing distance of 20 in).

[2]Hewlett-Packard Company, 3000 Hanover St., Palo Alto, CA 94304-1185.

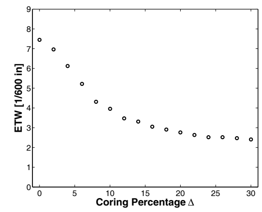

Figure 4. *ETW as a function of coring percentage Δ for lines with $\Omega = 10/600$ in and colorant content C = M = 100%, Y = K = 0%. As Δ increases, ETW decreases.*

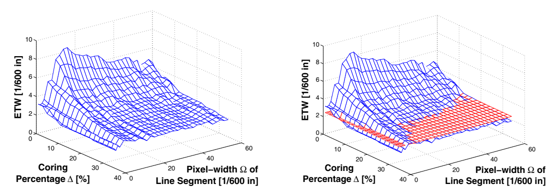

(a) (b)

Figure 5. *(a) ETW (blue surface) as a function of coring percentage Δ and line width Ω, measured from test pages printed with C = M = 100%, Y = K = 0%. (b) Same plot as in (a) with the absolute blur detection threshold of the human visual system shown as red plane.*

Blur will be perceived consistently by the average human viewer on those lines whose width Ω and coring percentage Δ correspond to points on the surface above the absolute threshold plane (4×10^{-3} in). For each line width, the optimal coring percentage is given by the smallest coring value for which the ETW is smaller than 4×10^{-3} in, assuming that the ETW decreases as coring increases. The intersection of the detection threshold plane and the ETW surface results in a level curve that marks the boundary between what is perceived as blur and what is not. The optimal coring percentage Δ_{OPT} for each line width Ω is the value of the coring Δ at that level curve, as illustrated in Fig. 6(a). The optimal coring percentages Δ_{OPT} for each line width Ω are plotted in Fig. 6(b). For regions wider than 60/600 in, a coring strategy slightly more conservative than the one chosen for the range 42/600 in - 60/600 in should be implemented.

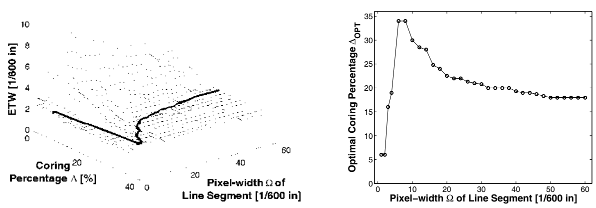

(a) (b)

Figure 6. *(a) The optimal coring percentage $\Delta_{\rm OPT}$ for each line width Ω is determined by the level curve that results from the intersection (shown by the heavy solid line) between the ETW surface and the detection threshold plane. (b) Level curve shown in (a) by heavy solid line, but plotted as coring percentage Δ vs. line width Ω. This specifies the optimal coring percentage $\Delta_{\rm OPT}$ as a function of line width Ω.*

Memory Efficient Coring Algorithm

Any algorithm designed to run within the printer's imaging pipeline must adhere to the limitations imposed by the hardware architecture. For the memory efficient coring algorithm, this implies that it should process the image in raster order and should require the storage of only a few lines of data at a time (eg. five lines of the 600 dpi image). At this point, however, we know that an optimal coring algorithm must be capable of estimating the dimensions of the line/edge structure, since the way in which those structures are modified depend on their size as well as on their colorant content. This might be difficult, if not impossible to achieve with only 5 image lines available at the same time.

Fortunately, the image pipeline provides additional resources that are indispensable to the task at hand. In order to facilitate storage of the image data, the high resolution image data is compressed before being sent to the laser subsystem for printing. Generally, the compression schemes applied are similar to the JPEG sequential encoding mode. Specifically, the high resolution image is processed on a block-by-block basis in raster scan order. The relevant implication of this approach is that, in addition to the 5 lines of CMYK high resolution data, low resolution information about the image is also available at any given time. Assuming that the block size used in the compression scheme is 8×8 pixels, and taking into account the storage capacity of the engine's buffer, 9 lines of 75 dpi CMYK image data can be made available to the coring algorithm. The main concept behind the algorithm is to use both the high resolution and the low resolution image information to estimate the dimensions of the image structures, thus allowing for the application of the optimal coring percentages found in the previous section.

Figure 7 shows a block diagram that illustrates the operation of the coring algorithm. The algorithm processes the high resolution CMYK data in raster order and first determines whether the combination of colorants at each pixel is one known to produce toner scatter around edges. The pixel is processed only if it possesses such a concentration of CMYK, and if it is not an edge pixel. Recall that a two-pixel wide edge is left unchanged by the selected coring technique. If it is an interior point, the dimensions of the region in which the pixel is located are found.

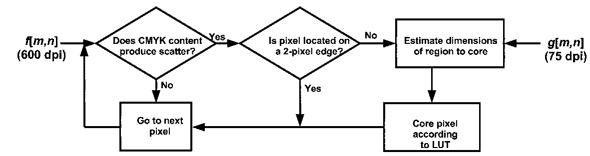

Figure 7. *Block diagram for coring algorithm.*

The model for toner overdevelopment is based on measurements of lines with different widths and colorant content. Consequently, the output of the dimension estimating step of the coring algorithm needs to be relatable to the line width parameter on which the characterization stage was based. The line width can be seen as the length of the shortest path that goes from one side of the line to the opposite side. The coring algorithm estimates the dimension of the region in which the pixel is located by calculating the length of several straight paths across the region and finding the traversing path with the shortest length. Each of the paths emanate radially from the position of the pixel being processed.

Figure 8 illustrates how the dimensions of the region in which the processed pixel lies are determined. Figure 8(a) shows a portion of the C plane of the original 600 dpi image, with the pixel being processed and its corresponding 5×5 pixel window highlighted. Figure 8(b) shows the corresponding 75 dpi image, scaled for visualization purposes to the same size as the high resolution image. The 9×9 window surrounding the pixel being processed is also indicated. The effective width $\Omega_{\rm EFF}$ of the region is defined as

$$\Omega_{\rm EFF} = \min\{L_i, i = 0, 45, 90, 135\}, \qquad (3)$$

where the L_i are the lengths of the paths represented by the dashed arrows in Fig. 8(b) for each of the angles $i = 0^o$, 45^o, 90^o, and 135^o and are calculated as follows:

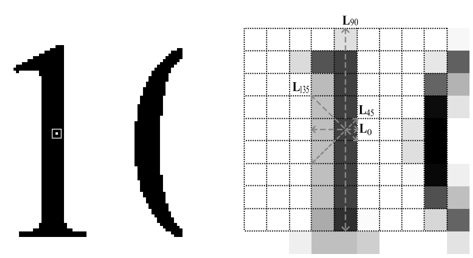

(a) (b)

Figure 8. *Calculation of effective line width: (a) C plane of a 600 dpi image, pixel being processed and 5×5 pixel window. (b) Corresponding 75 dpi image obtained by averaging blocks of 8×8 pixels in the 600 dpi image. The dotted lines indicate the 9×9 low resolution window used to estimate the dimensions L_i. The effective width of the region is $\Omega_{\rm EFF} = \min\{L_i, i = 0, 45, 90, 135\}$.*

1. Let the colorant content of the pixel being processed be $0 \leq C_0 \leq 1$. Initialize the length counters $L_i = L_{i+180^o} = 0$.

2. Traverse the path emanating at an angle i from the position of the pixel being processed in the low resolution image until a white pixel is found or until the end of the 9×9 window is reached. At each pixel, increase L_i by $8 \times C/C_0$, where C is the value of the low resolution pixel.

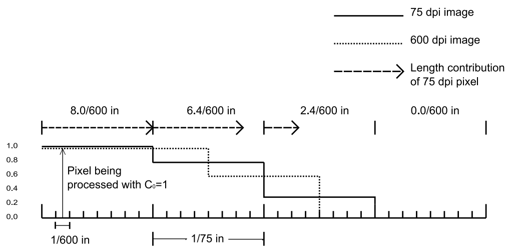

Figure 9. *1-D illustration of length estimation. The small tick marks on the x-axis indicate the boundaries between the pixels in the 600 dpi image, while the large tick marks indicate the boundaries between the pixels in the 75 dpi image. The gray levels of the 75 dpi image (solid line) are calculated by averaging the gray levels of the 600 dpi image (dotted line) across blocks of* 8×8 *pixels. The contribution of each pixel in the 75 dpi image to the overall length of the path is equal to* $8/600$ *in times the ratio of the gray level of the 75 dpi pixel to the gray level of the pixel being processed. The lengths of the dotted arrows indicate the contribution of each 75 dpi pixel to the length of the path. In this case, the leftmost pixel in the 75 dpi image with a gray level of 1 contributes* $1 \times 8/600$ *in to the length of the path while the adjacent pixel, which has an average gray level of 0.8, contributes* $0.8 \times 8/600$ *in to the length of the path.*

3. Repeat Step 2 for the angle $i + 180^o$ and let $L_i = L_i + L_{i+180^o}$.
4. Let $L_i = k_i \times L_i$, where
$$k_i = \begin{cases} 1 & \text{if } i = 0 \text{ or } i = 90, \\ \sqrt{2} & \text{if } i = 45 \text{ or } i = 135. \end{cases}$$

Once the width information of the region is available, it is straightforward to determine the optimal amount of coring by consulting a lookup table containing Δ_{OPT} values for different colorant combinations and line widths. Note that the maximum region width that can be measured with the available resources is 72 pixels. Regions wider than 72 pixels will be left unchanged, while the coring percentage for regions with effective width in the range from 60 to 72 pixels will be determined by linear interpolation between the corresponding entry in the lookup table at 60 pixels and 0% coring at 72 pixels.

Results

The coring algorithm described in the previous section was applied to multiple documents containing mainly text and solid areas. Since the impact of the algorithm is most noticeable around edges, the results shown in this section focus on those critical areas. Figure 10 shows the result of applying the coring algorithm to the 12 point Times New Roman characters “e” and “o” with colorant content C = M = 100%, Y = K = 0%. It can be seen that the toner scatter is greatly reduced in the text processed by the algorithm, thus yielding the appearance of sharper edge transitions.

Figure 11 shows the result of applying the coring algorithm to a 60/600 in wide line with colorant content C = M = 100%, Y = K = 0%. Figure 11(a) shows a captured version of the printed line without coring, while Fig. 11(b) shows the scanned version of the same line after coring. It is evident that while the effect of toner scatter is not as critical on wide lines, the coring algorithm still improves the sharpness of the transitions.

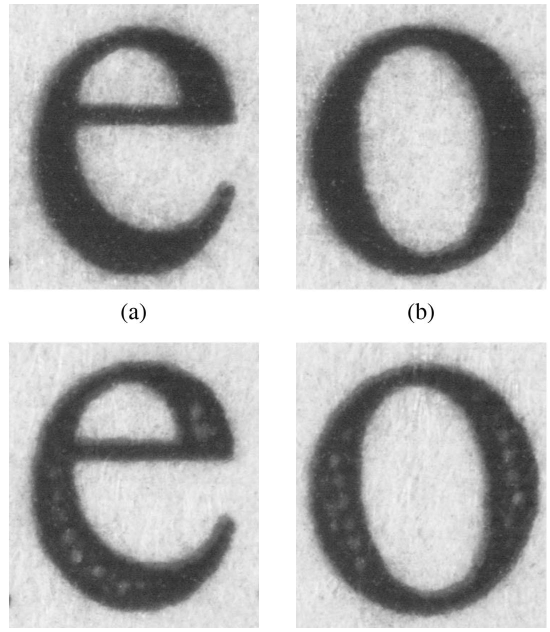

(a) (b)

(c) (d)

Figure 10. *Images of 12 point Times New Roman characters with colorant content C = M = 100%, Y = K = 0%: (a) letter “e” before coring, (b) letter “o” before coring, (c) letter “e” after coring, and (d) letter “o” after coring. The coring algorithm decreases toner scatter surrounding edges. Captured at 5000 dpi, with luminance channel only.*

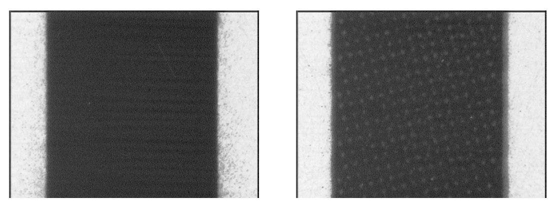

(a) (b)

Figure 11. *Images of a 60/600 in wide edge with colorant content C = M = 100%, Y = K = 0%: (a) before coring, (b) after coring. The coring algorithm decreases toner scatter surrounding edges. Scanned at 5000 dpi, with luminance channel only.*

One of the approaches currently implemented for correction of toner scatter in existing products consists of clipping the color gamut of the printer by limiting the possible colorant combinations via conservative color tables. Figure 12 shows a comparison between the output of the color clipping approach and the coring algorithm. Figure 12(a) shows a sample scanned image of a $300/600$ in $\times$ $1000/600$ in line with C = M = 100%, Y = K = 0% colorant content rendered through the clipping color table. Figure 12(b) shows a sample scanned image of the same line printed through a color table that does not perform color clipping. Figure 12(c) shows a sample scanned image of the same line printed through the same color table as in (b) but after the coring algorithm has been applied. It can be seen that while both the color clipping and the coring algorithm make edges sharper, the former does so at the expense of larger color and texture differences. With the clipping solution, the halftone textures are clearly visible and the color error incurred is 15.2 ΔE units[3] with respect to the uncorrected image. On the other hand, the textures on the cored image are hardly visible and the color error is only 2.5 ΔE units.

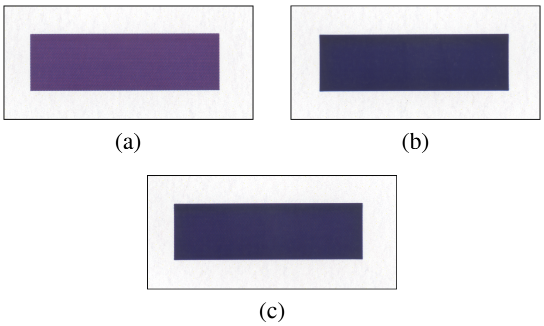

Figure 12. *Comparison of the current solution and the proposed solution to toner scatter. The images are scanned versions of a* $300/600$ *in* $\times$ $1000/600$ *in line with C = M = 100%, Y = K = 0% colorant content, (a) printed after colorant clipping, (b) printed without colorant clipping, and (c) printed after coring has been applied. Even though both the colorant clipping approach and the coring algorithm manage to reduce toner scatter, the former does so at the expense of color and texture errors. Scanned at 600 dpi.*

Conclusions

We developed a memory efficient algorithm to reduce the scattering artifacts introduced near the edges of text, lines, and solid color blocks by the development stage of the electrophotographic process below the threshold level that has been found to be perceivable by human beings. We successfully applied the algorithm to multiple types of documents containing text and graphics. The proposed solution for scatter correction outperforms the existing solution in terms of color and texture preservation. While the proposed approach was applied to one particular colorant combination, it can be generalized to any combination that is known to cause blurriness due to toner scatter.

Acknowledgements

This research was supported by the Hewlett-Packard Company. It was conducted while Edgar Bernal was a graduate student at Purdue University.

References

[1] ISO/IEC 13660:2001. Information technology – Office equipment – Measurement of image quality attributes for hardcopy output – Binary monochrome text and graphic images.

[2] J. Grice and J. P. Allebach, The Print Quality Toolkit, J. Imaging Sci. and Technol., 43, 2, (1999).

[3] E. N. Dalal et. al., INCITS W1.1 Standards for Perceptual Evaluation of Text and Line Quality, Image Quality and System Performance, pg. 34, (2004).

[4] W. Wu and E. N. Dalal, Perception-based Line Quality Measurement, Image Quality and System Performance II, pg. 111, (2005).

[5] T. Itoh and S. Hirota, Evaluation of Legibility, Proc. PICS, pg. 213, (1999).

[6] T. Itoh and S. Hirota, Evaluation of Legibility using Line Reproduction Quality and MTF, J. Imaging Sci. and Technol., 43, 5, (1999).

[7] C. A. Dvorak and J. R. Hamerly, Just-Noticeable Differences for Text Quality Components, J. Applied Photographic Eng., 9, 3, (1983).

[8] M. Sato, Analysis of Quantitative Indicators of Kanji Text Quality, Proc. PICS, pg. 218, (1999).

[9] J. R. Edinger Jr. and C. Newell, Subjective Impression of the Weight of Text Correlates with Measured L-Width, J. Imaging Sci. and Technol., 41, 2, (1997).

[10] J. R. Hamerly and C. A. Dvorak, Detection and Discrimination of Blur in Edges and Lines, J. Optical Soc. of America, 71, 4, (1981).

[11] L. Schein and G. Beardsley, Offset Quality Electrophotography, J. Imaging Sci. and Technol., 37, 5, (1993).

[12] L. B. Schein, Electrophotography and Development Physics, Laplacian Press, Morgan Hill, CA, 1996.

[13] E. M. Williams, The Physics and Technology of Xerographic Processes, Krieger, Malabar, FL, 1993.

[14] N. Burningham, J. P. Allebach and Z. Pizlo, Image Quality Metrics, Encyclopedia of Imaging Science and Technology, Wiley, New York, NY, 2002, pg. 598.

[15] R. Eschbach, R. Bala and R. deQueiroz, Simple Spatial Processing for Color Mappings, J. Electronic Imaging, 13, 1, (2004).

[16] R. Bala and R. Eschbach, Spatial Color-to-Grayscale Transformation Preserving Chrominance Edge Information, Proceedings of the 12th Color Imaging Conference, pg. 82, (2004).

Author Biography

Edgar Bernal received his BSEE from Pontificia Universidad Javeriana in 1999 and his M.Sc. and Ph.D. degrees from Purdue University in 2002 and 2006 respectively. He has worked at the Xerox Research Center in Webster, NY since September of 2006.

Jan P. Allebach received his BSEE from the University of Delaware in 1972 and his Ph.D. from Princeton University in 1976. He was on the faculty at the University of Delaware from 1976 to 1983. Since 1983, he has been at Purdue University where he is Hewlett-Packard Professor of Electrical and Computer Engineering. Allebach is a Fellow of the IEEE, IS&T, and SPIE. In 2007, he was named Honorary Member of IS&T, the highest award that the Society bestows on its members.

Jeff Trask received a Master of Engineering in Mechanical Engineering from Brigham Young University in 1981. Since 1981, he has been employed in Boise, Idaho by the Hewlett-Packard Company as a color printer R&D engineer. Most recently, he worked on the HP Color LaserJet CP1515n product. His current position is Color Print Quality System Architect.

[3] CIE 1976 $L^*a^*b^*$ with D65 illuminant and 2^o observer.